Journal of Magnetism and Magnetic Materials 475 (2019) 14–23

Contents lists available at ScienceDirect

Journal of Magnetism and Magnetic Materials

journal homepage: www.elsevier.com/locate/jmmm

Research articles

Drug targeting investigation in the critical region of the arterial bypass graft

Sandor I. Bernad[a,*], Daniela Susan-Resiga[a,b], Ladislau Vekas[a,*], Elena S. Bernad[c]

[a] Centre for Fundamental and Advanced Technical Research, Romanian Academy, Timisoara Branch, 300223 Timisoara, Romania
[b] West University of Timisoara, Faculty of Physics, RO-300222 Timisoara, Romania
[c] University of Medicine and Pharmacy "Victor Babes" Timisoara, RO-300041, Romania

ARTICLE INFO

Keywords:
Magnetic particle targeting
Bypass graft
Particle deposition
Hemodynamics

ABSTRACT

Magnetic targeting is a non-invasive strategy to improve treatment efficacy for graft intimal hyperplasia (the leading cause of the arterial bypass graft failure). The present study aims are to investigate the possibility of MPs retention in the bypass graft anastomosis region where IH are developed after surgical intervention and quantify the particles accumulation function of the position of the external magnetic field. In this study iron (Fe) particles with 10 μm in size were used to model the magnetic carrier mixed in the glycerol-water solutions. The 10 μm diameter iron particle was used only to model the magnetic carrier in experimental investigation (not intended for clinical use), to demonstrate the feasibility of the particle targeting. Magnetic fields are generated by NdFeB external magnet. Positioning permanent magnet near to the diseased area resulted in a deviation of the injected ferromagnetic particles within the blood flux and their capture onto the wall of the bypass graft test section. To increase the accumulation of the particles in the targeted region, it is critical to understand the effect of the flow structure on particle deposition, namely interaction between the instabilities formed in the primary vortex of the anastomosis region. The results presented in this paper, put in evidence the blood constituents migrations to the artery wall for the specific flow pattern (through used iron particles), and demonstrate the feasibility of the magnetic drug targeting as a potential alternative method for effective treatment of the bypass graft intimal hyperplasia.

1. Introduction

Arterial or vein bypass grafts with single proximal and multiple distal anastomoses are often used in patients undergoing coronary artery bypass graft (CABG) surgery [1].

Bypass graft remodeling is a complex process involving hemodynamic and biological factors. Following CABG surgery, bypass graft failures are classified either as early (cause of graft failure is thrombosis) or late (cause is the neointimal hyperplasia – IH).

Many data from the literature indicate that in the anastomosis configuration, the IH occurs preferentially around the suture line, the toe, and the heel regions. Change of the hemodynamic conditions after surgical intervention induce a change in the flow pattern. This changes in flow pattern have directly correlated with the migration of the wall shear stress value in the pathologic range [2–4].

For example, one of the main conclusions of the PREVENT IV trial (PREVENT-IV was a phase-3, multicenter, randomized, double-blind, trial to prevent neointimal hyperplasia and vein bypass graft failure). This conclusion refers to the additional studies to better understand the most appropriate conduit of the flow pattern to improve long-term graft patency and clinical outcome of patients undergoing CABG surgery [5].

Magnetic targeting is an attractive non-invasive strategy to improve treatment efficacy for graft intimal hyperplasia. In the current practices, this remains a challenge, until both, techniques and used drugs achieve some desired characteristics like drug durability, drug non-toxicity and drug release in a controlled manner [6–8].

Our previous work was focused on two distinct directions, namely to the potential application of the magnetic drug targeting for treatment of the intimal hyperplasia in the arterial bypass graft [9], and to investigate and analyze the blood hydrodynamics in the bypass graft anastomosis region for different type of graft geometry (straight and helical geometries) [10,11].

The post-interventional natural behavior of the bypass graft differs significantly from native vessels inducing higher risk for restenosis. Loss of the graft patency and the risks of repeat surgery are not negligible aspects for the long-term bypass graft evolution. In the current medical practices in the majority of case, percutaneous intervention is the preferred therapeutic modality for treatment of the graft failure (involving stent placement, bare-metal stents – BMS or drug-eluting stents – DES) [12]. Unfortunately, percutaneous intervention is associated with a

* Corresponding authors.
E-mail addresses: sandor.bernad@upt.ro (S.I. Bernad), vekas.ladislau@gmail.com (L. Vekas).

https://doi.org/10.1016/j.jmmm.2018.11.108
Received 7 May 2018; Received in revised form 19 November 2018; Accepted 22 November 2018
Available online 23 November 2018
0304-8853/

high rate of the major adverse cardiac event irrespective of the implanted stent type (restenosis and thrombosis) [13].

Traditional local delivery systems of the drug (like drug-eluting stents) have been shown to lack sustained delivery and adverse the event. Therefore, magnetic drug targeting represents a potential alternative for prolonged local delivery of therapeutic agents [12].

For example, Pislaru et al. [14] investigated endothelialization of the synthetic vascular grafts (8 mm diameter Dacron grafts) using superparamagnetic microspheres (SPMs) (0.9 mm diameter, coated iron oxide particle) in the presence of the magnetic force. Authors conclude that endothelial cells loaded with SPMs are rapidly captured and retained on the Dacron graft surface under pulsatile flow conditions.

The present study aims, are to investigate the possibility of the magnetic particles (MPs) retention in the realistic post-surgical bypass graft anastomosis region (30-degree bypass graft angle) and quantify the particles accumulation, function of the position of the external magnetic field.

Because flow velocity in the circulatory system is not a controllable parameter, the dependence of magnetic control efficiency on flow velocity determines the size of blood vessels in which drug targeting is practical. We assume steady flow but use realistic mean velocity values for blood flow in the artery. The analysis is not meant to accurately model magnetic drug targeting in the artery (particles sticking to vessel walls both in proximal and distal sections of the targeted region), but rather to find realistic ranges for a set of parameters that will be used in further simulations and experiments.

2. Experimental setup

Experimental setup used for particle trapping is shown in Fig. 1 (this setup described in detail in our previous work [9]).

Magnetic particles were injected into the main flow upstream of the bypass graft inlet section. The syringe pump was used to push the carrier fluid into the main flow. Injecting the particles (suspension) at a distance of 2D (D – graft diameter) before the graft inlet section, facilitated dispersion of them in the fluid flow stream at the entrance of the graft.

The measurements procedure used for investigation was:

1. The main flow was turned on and adjusted up to 0.2 m/s, corresponding to 602 mL/min flow rate (0.2 m/s is the average blood velocity corresponding to the patients without significant stenosis, minimum velocity of 0.15 m/s and maximum velocity of 0.28 m/s, [15]).
2. The position of the permanent magnet is adjusted to the desired distance from the bottom wall of the anastomosis region.
3. The syringe pump injected the carrier fluid contained MPs into the main flow in interval time of the 30 s. We used this time interval to avoid sedimentation of iron particles in the syringe pump, respectively to be able to quantify the flow effect on the particle deposition in the anastomosis region.

Particle distribution and the flow field in the anastomosis region was investigated using the image analysis technique. To visualize both flow dynamics and particle depositions a Sony XC CCD camera was used to record the investigated processes.

2.1. Graft geometry

Realistic anastomosis is variable regarding graft/artery calibers, graft angle, flow rates, and out-of-plane curvatures. In the real anastomosis geometry (Fig. 2A) the low wall shear stress (WSS) covers, the artery floor opposite the graft orifice, the lateral wall of the graft–artery interface, the zone distal to the toe, practically the zone where the intimal hyperplasia develops. Our test section is a copy of the realistic post-surgical bypass graft anastomosis region for the bypass graft with of the 30° anastomosis angle.

The test sections with the anastomotic angle of 30° are fashioned into a right shape from glass tubing, with a constant internal diameter of 8 mm (Fig. 2B). Flow experiments were conducted under typical physiological conditions [15]. The mean flow velocity is $U_m = 0.2$ m/s, corresponding to the Reynolds number of Re = 471 (based on graft diameter and fluid viscosity).

2.2. Blood analog fluid preparation

Drug carriers are used to deliver the drugs in a controlled manner to the target artery site (bypass graft anastomosis in our case). Working fluid used for this analysis is a blood analog fluid, which has the density (ρ) same to the blood of 1060 kg/m^3.

Because the flow considered in this study are steady and contain only very small regions with shear rates lower than 10 s^{-1}, the blood viscosity model does not include viscoelasticity [9,11,16].

2.2.1. Rheological properties of the blood analog fluid

For blood analog carrier fluid (CF), glycerol-water solutions prepared by mixing calculated weights of distilled water and glycerol. Glycerol is a colorless, viscous, liquid with a density of 1.26 g/cm^3 and is miscible with water [17].

Viscosity curves at T = 25 °C, respective T = 37 °C of carrier fluid presented in Fig. 3 indicates a shear-thinning behavior (typical of pseudoplastic systems) at low shear-rates, which becomes Newtonian at shear rates > 10 s^{-1}.

In this paper, in order to evaluate the hydrodynamic graft performances, ferromagnetic particles (FMP's) were utilized for quantification of particle deposition in the anastomotic region. The iron particles suspension in glycerin–water mixture carrier is a magnetorheological fluid (MR fluid) [18]. Bio-ferrofluids with a multicore magnetic particles-potential magneto-responsive drug carriers-show significant magnetoviscous effect similar to MR fluids [19].

The model suspension of magnetic carriers used in experiments was obtained mixing blood analog carrier fluid (CF) (aqueous glycerol solutions) with iron (Fe) particle (10 μm in size, Merck KGaA, Darmstadt,

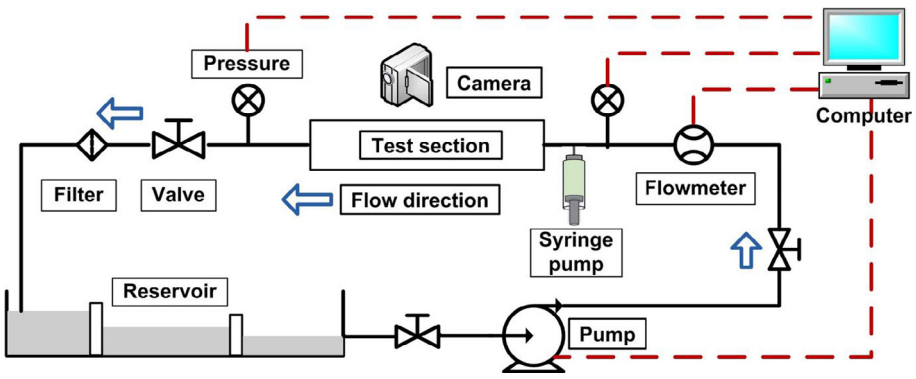

Fig. 1. Experimental setup used for bypass graft investigations. The block diagram of the main recirculating flow loop contained: flowmeter, particle injection mechanism – syringe pump, test section – bypass graft model, valve, particle filter, reservoir, centrifugal pump. Syringe pump injects suspension in front of the bypass graft entry section.

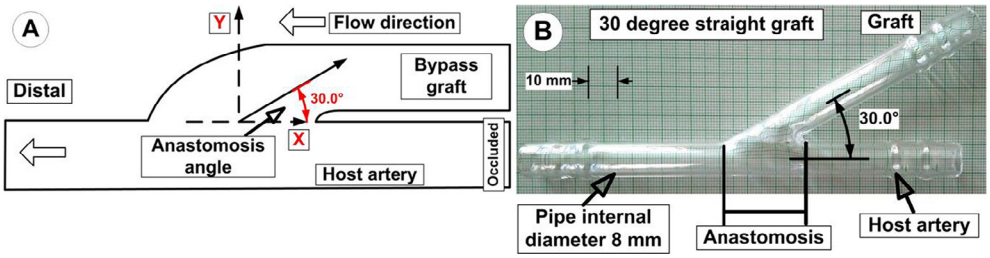

Fig. 2. A) Definition of the anastomosis angle after to the bypass graft surgery intervention. B) Simplified experimental bypass model fashioned in a straight shape from the glass tube with a constant internal diameter of 8 mm (both, graft and host vessel).

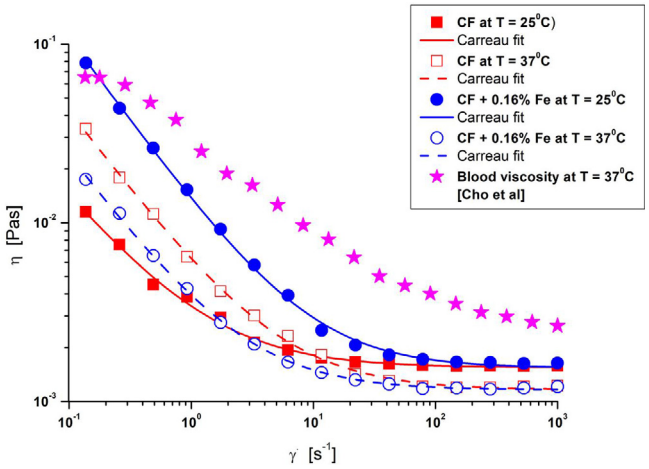

Fig. 3. Comparison between the viscosity curves of the carrier fluid (CF), the used suspension fluid (CF + 0.16% ferromagnetic particles) and blood, for different working temperatures.

Germany) with 0.16% mass concentration.

The degree of change in the model suspension depends on the magnitude of the applied field. The fluid structure further depends on the volume fraction such that dilute suspensions form in the magnetic field some weakly interacting single particle chain, while more strong system forms particle chains cross-linked laterally into a dense network. Magneto-viscous characteristics were measured using a rotational rheometer (MCR 300, Physica, Stuttgart, Germany).

Fig. 3 shows that the Fe particle suspensions exhibit shear-thinning behavior in the absence of the magnetic field, probably due to the shear-thinning character of the carrier fluid at low shear rates, and to the small aggregates of the Fe microparticles, that are progressively destroyed with shear intensification. The rheological values for the aqueous glycerol solutions presented in Table 1, can be described using the Carreau model with four fit parameters Eq. (1) [20,21].

$$\eta(\dot{\gamma}) = \eta_{\infty} + (\eta_o - \eta_{\infty})[1 + (C\dot{\gamma})^2]^{-p} \quad (1)$$

where η_0 is zero shear viscosity, η_∞ is the viscosity at infinite shear rates, C is the characteristic time constant, and p is the flow behavior index.

Table 1
Rheological characterization of the carrier fluid and Fe particle suspensions.

Fluid	t [°C]	B [mT]	η_o [Pa s]	η_o [Pa s]	C [s]	p [–]	R^2
CF (aqueous glycerol solutions)	25	0	0.0015	0.026	4.66	0.785	0.909
	37	0	0.0012	0.023	4.38	0.812	0.998
CF + 0.16% Fe	25	0	0.016	0.174	15.69	0.475	0.998
	37	0	0.013	0.131	16.46	0.552	0.995

The R^2 values for all fits are close to the unity, indicating an excellent fit (R^2 – is the coefficient of determination used to evaluate quality of the Carreau fits).

The values of the fit parameters obtained to fit the experimental data from Fig. 3 are presented in Table.1. The comparison of the used suspension viscosity and the real blood viscosity presented in [22] shows a good agreement (Fig. 3).

It is important to mention that wall shear stress (WSS) is dependent on the fluid viscosity and the gradient of the velocity profile perpendicular to the vessel surface (practically derived from the friction of the flowing blood on the endothelial surface of the arterial wall). In the present paper, we investigated the particle targeting possibilities for the WSS value in a pathologic and normal range corresponding to the blood flow in the arterial bypass graft [23,24] (Fig. 3).

2.2.1.1. Magnetic particle characterization. In this study, Fe particles with 10 μm in size (Merck KGaA, Darmstadt, Germany) were used to model the magnetic carrier (Table 2). The particles size is much larger than those used for drug delivery [25,26], but are comparable to the size of circulating cells such as red blood cells (RBC) and platelets (human RBCs is 1.7 μm to 2.2 μm in thickness and approximately 7.5 μm to 8.7 μm in diameter [27]).

Practically, this type of magnetic particles was chosen, for its commercial availability, but rather due to the results obtained by Pislaru et al. [14], for endothelialization of the 8 mm diameter synthetic vascular grafts (commercial Dacron grafts) used the 0.9 mm diameter coated iron oxide particle (a large diameter particle).

It is important to mention that we used the 10 μm iron particle as a model to demonstrate the feasibility of the magnetic drug targeting in the bypass graft (this type of particles does not intend to use in clinical practices).

Physical morphology of the used Fe particles was confirmed via microscopic image presented in the Fig. 4.

Magnetic properties of the magnetic carrier (Fe particles) were measured using a vibrating sample magnetometer – VSM 880-ADE Technologies, USA, at room temperature (22 °C), in the field range of 0 kA/m to 950 kA/m. Fig. 5 shows the full magnetization curves and hysteresis loops of the samples. As can see in Fig. 5, the hysteresis loops are smooth and no hysteresis, which indicated a soft magnetic material with coercive force and the residual magnetization approach to zero (Table 3).

Table 2
Fe characteristics, used in the experiments.

Characteristics	Value
- Particle diameter	10 μm
- Density	7.87 g/cm^3
- Molar mass	55.85 g/mol
- Chemical composition	in mass concentration percentage: Fe-99.5%; S-0.002%; Cl-0.002%; As-0.0002%; Cu-0.002%; Pb-0.002%; Mn-0.002%; Zn – 0.002%; other-0.1%.

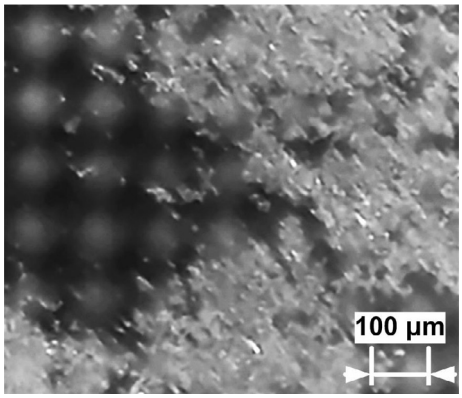

Fig. 4. Microscopic image of the 10 µm Fe powder morphology.

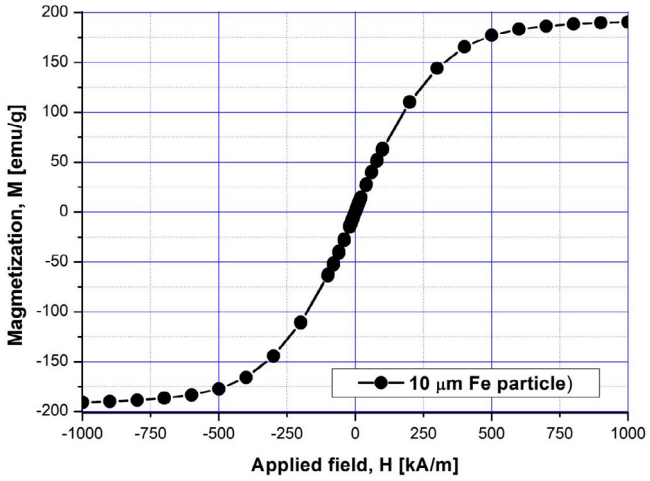

Fig. 5. Magnetization curve measured in a powder state of micro-sized (10 µm) Fe particles.

Table 3
Fe particle magnetic properties (particle size of 10 µm).

Saturation magnetization	Saturation field	Coercive field	Remanent magnetization
Ms [A·m^2/kg] – 190	Hs [kA/m] – 563	Hc [kA/m] – 0.81	Mr [A·m^2/kg] – 0.562

3. Magnetic targeting

The magnetic drug targeting (MDT) involves exposure of the area of interest (targeted region) to an externally applied magnetic field, followed by the administration of magnetic particles. After administration (injection during a specific time), particles were delivered to the area of interest by the fluid flow.

The significant limitations of the MDT consist in low retention of the MNP's due to the reduced value of the magnetic force comparatively with the hydrodynamic force acting in the circulatory system.

In the next sections, we present our results regarding magnetic drug targeting possibilities and efficiency applied for treatment of the arterial bypass graft anastomosis region.

3.1. Magnetic field generation

Usually, the magnetic fields are generated by external magnets. The magnetic induction for in-vitro studies varies from ≈70 mT to ≤1.5 T [28] and for animal trials between 0.1 and 1.5 T [29,30].

To obtain the magnetic field gradient, we first took measurements of the magnetic flux density within a region of interest (L × W × h = 26 mm × 29 mm × 5 mm) perpendicular to the pole face of the test magnet (Fig. 6A). Fig. 6B is a plot showing the magnetic field induction B within the measurement range, along with the different vertical distance of the magnet surface. The permanent magnet we used was a NdFeB magnet, the most widely-used type of rare-earth magnet [31].

To investigate the magnetic field generated by the NdFeB30 magnet, we ran the simulation using freeware – Finite Element Methods Magnetics (FEMM) (http://www.femm.info/wiki/HomePage). The NdFeB30 magnet (or commercial notation N30 – Neodymium 30) represent the NdFeB permanent magnet from the rare earth family magnet with maximum energy product (BxH) of 30 MGOe. To evaluate the magnetic field gradient in a section of interest, we set up a 2D problem by simulating the longitudinal section of the investigated setup (both, the test section – bypass graft, and the used permanent magnet) as shown in Fig. 7.

When the distance between the permanent magnet and the vessel wall is small, the gradients of the magnetic field are high ($> 0.1\ \mathrm{T\,cm^{-1}}$, Figs. 6B and 7), and the MPs can be captured from the flow field in the targeted region and enable stable deposit. As expected, if the distance is considerable (small magnetic field gradients is present) the chance of magnetic capture is small, and MPs, are flushed out from the targeted region.

4. Results and discussion

4.1. Flow hydrodynamics

Real human arteries are tortuous and induce secondary flows, defined as velocity components that are not parallel to the local tube axis. From the arterial flow point of view, it is essential to determine whether secondary flows change the shear-dependent viscosity variation.

During the flow through the bypass graft, the generated inertial and circumferential forces imposed a change in fluid flow direction. As can see in Fig. 8A, downstream to the stagnation point, a strong double helicoidal flow developed, consists in a pair of a secondary spiral flows located distal to the toe (Dean type vortices). This type of vortices can be identified clearly in Fig. 8B. The presence of these vortices in the bypass graft is in agreement with cases reported in the literature and also in our previous results (obtained after numerical and experimental investigations of the 45°bypass graft) [9,11].

This abnormal flow field is characterized by flow separation at the toe, strong flow impact on the host artery floor and flow oscillation in the bypass graft anastomosis region. Generated secondary flows produce complicated distributions of shear rate, which may produce unexpected effects of shear thinning [9]. Secondary flows also produce axial vorticity, which is not present in parallel flows [10,16].

4.2. Experimental magnetic particle deposition

For this section, the questions are: a magnetic particle can be directed to target a specific region of the coronary bypass graft? So, consequently where the particles will accumulate?

To answer these questions, we suppose a simple scenario: steady-state flow, straight bypass geometry with 30-degree anastomosis angle, and spatially varying magnetic forces.

The central assumptions for the experimental investigations of the flow are steady laminar flow, negligible gravitational effects, and constant physical properties.

In our experiment, particles have around the 10 µm diameter. Particles are essentially inertia-free, so the difference between the velocity of the particles and the velocity of the flow around them is negligible. Consequently, hydrodynamic interactions between particles are negligible. It this paper we consider only magnetic interparticle forces and ignore hydrodynamic interactions.

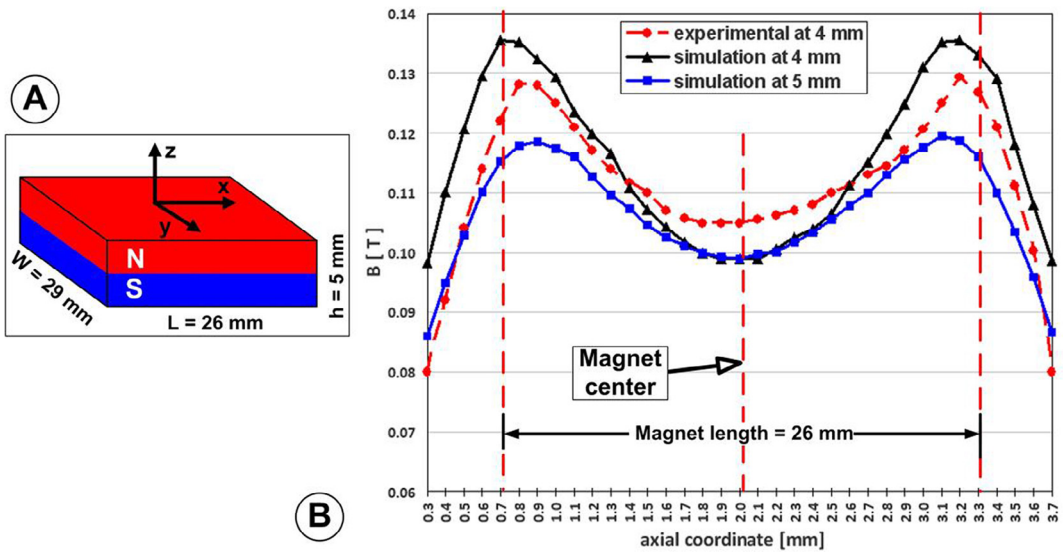

Fig. 6. A magnetic field generated by the NbFeB30 permanent magnet used in the experimental investigation. A). The dimension of the used magnet and axis association. The used permanent magnet has an axial polarization indicated in the figure. B). The magnitude of the magnetic field produced by the permanent magnet in the longitudinal section, along axis X at the 4 mm and 5 mm (bypass wall) distance from the magnet surface. Figure showing a comparison of the magnetic field measured with F.W. Bell Gaussmeter, model 5080, and the magnetic field obtained from numerical simulation. The plot shows that the numerical solution of the magnetic field agrees well with the experimentally measured values. The differences are due to the position of the gaussmeter hole.

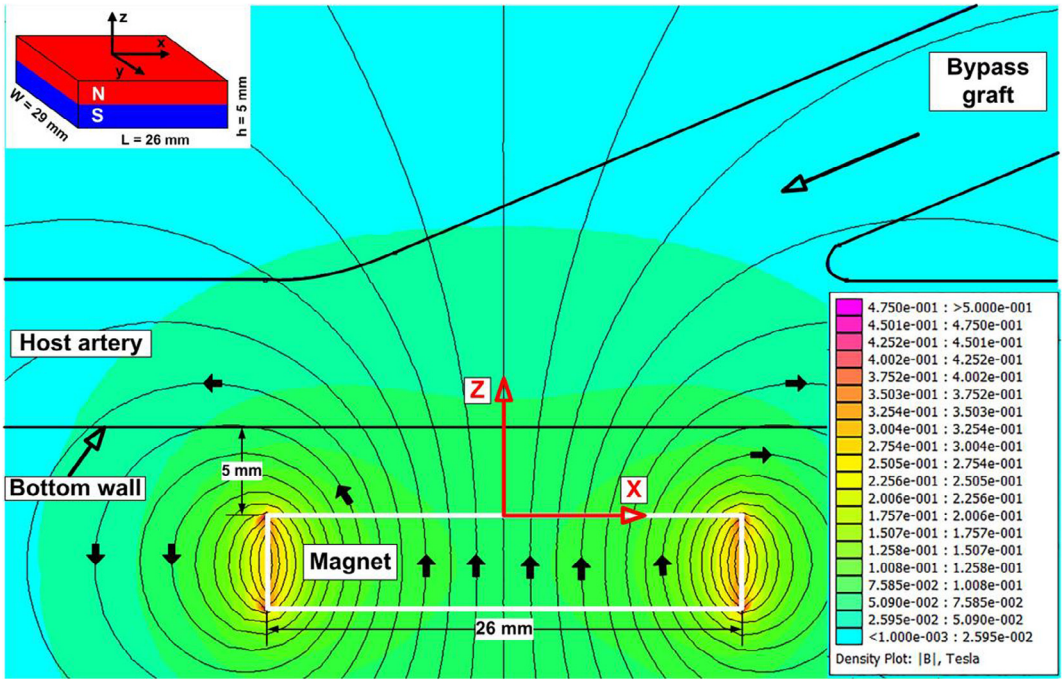

Fig. 7. A numerical simulation of the magnetic field used during the experimental investigation (free FEMM software was used). The figure shown the magnitude of the magnetic field produced by the NdFeB30 permanent magnet in longitudinal section, along to the bottom wall of the bypass graft at the distance of 5 mm from the magnet surface.

In our study, investigation of the particle depositions was for the following conditions (Table 4):

During the magnetic targeting, accumulation of the FMPs is the result of the action of several forces including magnetic forces from the applied magnetic field, hydrodynamic drag forces from the blood-stream, buoyancy forces, gravitational forces, and inertial forces. Because buoyancy forces, gravitational and inertial forces are several orders of magnitude lower than the magnetic force [9,32], these forces were considered negligible. In our work, the magnetic capture is based on the competition between the magnetic force exerted by the magnetic field gradient on the MPs and the drag force from the fluid (presented in detail in our previous work [9]). These forces act in opposition to each other and dictate de magnetic particles deposition in the anastomosis region (Fig. 9).

Consequently, in our case, the iron particle deposition occurs only where the magnetic force is of sufficient strength to counteract the drag force (Fig. 9).

Graft anastomosis geometry induces the local flow variation that determines the aspect of wall drug deposition and the extent and asymmetry of drug deposition.

Positioning permanent magnet near to the diseased area has obtained a deviation of the injected FMPs within the fluid flux and their

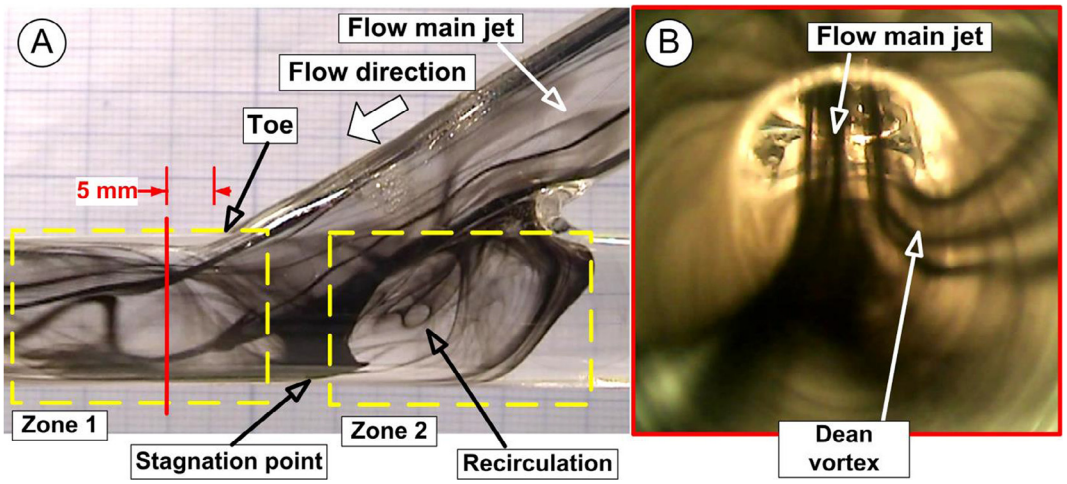

Fig. 8. Experimental flow visualization: (A) Flow dynamics in bypass graft with anastomosis angle of 30°. Vast recirculation region generated between occluded end and flow stagnation point. In the distal part of the host artery a helical type flow pattern was induced due to the interaction between main flow jet and the developed large recirculation region. (B) Flow visualization inside to the host artery distal to the anastomosis, using a 5 mm diameter endoscopic camera. Flow field corresponding to the section placed at the 5 mm distal of the anastomosis toe (red line in Fig. A). In this picture, we can see the generation of the Dean type vortex. (For interpretation of the references to colour in this figure legend, the reader is referred to the web version of this article.)

Table 4
Particle deposition parameters setup.

Parameters	Particle diameter	Mean flow velocity	Reynolds (Re)	Fluid viscosity	Magnetic field induction
Value	10 μm	0.2 m/s	471	0.0036 Pa s	0.07–0.13 T

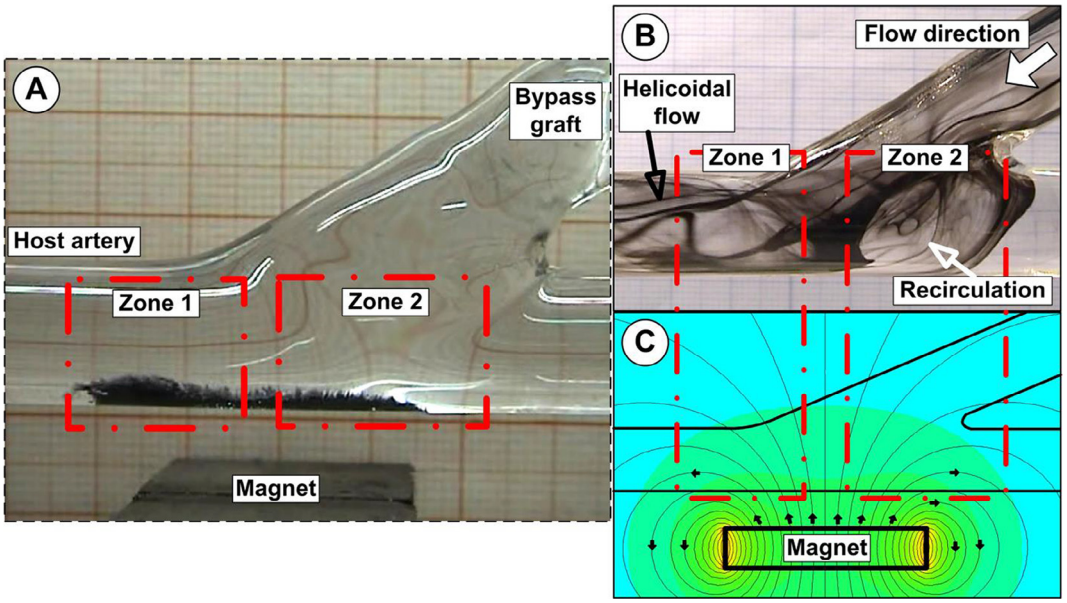

Fig. 9. A). The abnormal flow field is characterized by the flow separation at the toe, the strong flow impact on the host artery floor and flow oscillation at the heel region. The complex vortex structures created in the area between the heel and occluded part depends on the flow parameters and structure. B). Particle accumulations are based on the competition between the magnetic force and the drag force. This competition is correlated with the flow structure in the anastomosis region. As can see the presence of the two flow structures (zone 1 and 2) influence the deposition shape, and the quantity of the accumulated particles. Magnet distance from the bypass wall is 5 mm.

capture onto the wall of host vessels.

Taking into account that the distance between FMPs injection point (inlet section of the graft) and the bypass anastomosis is small practically after the time of 3 s the FMPs particle starts to deposit on the host tube wall (Fig. 9).

Fig. 9A and 9B show that fluid drag force acting on the FMP exceeds the magnetic forces generated by the magnet. In this situation, blood velocity washes the particles downstream to the anastomosis region before magnetic force affects particles. In the case of the comparable value of magnetic force and blood drag force, FMP build-up near the vessel wall creating a specific shape of the deposition (Fig. 9A).

Fig. 9 shows the variation in time of the FMP accumulation in the bypass anastomosis region for the constant position of the magnet (5 mm from the bypass bottom wall). For investigated geometry, particles accumulated in low lying “dunes” running across the entire pole face of the magnet and slightly increased accumulation downstream

from the stagnation point.

As it can be seen in Fig. 9A, a complex vortex structure is generated in the area between the heel and occluded part of the host artery. The primary vortex (zone 2), is the more significant vortex closest to the anastomosis, rotated anti-clockwise appeared to have a higher angular velocity. Generated angular velocity, induce to the fluid particles a periodically shedding from the central vortex into the graft flow (Fig. 9B).

For particles accumulation in the targeted region, it is critical to understand the effect of the flow structure on deposition. The instabilities formed in the primary vortex, disturb the incoming flow from the bypass graft inducing further fluctuations in the central vortex. More, the presence of active helical motion in the distal part of the graft (zone 1, Fig. 9B) increases the interaction between fluid, injected FMP particles, and the magnetic field. As a result, part of the injected particles is carried downstream in the host artery (zone 1 in Fig. 9A), and part of particles become trapped in the low shear stress regions of the artery wall (Fig. 9A and 9B).

Also, the presence of the recirculation flow (zone 2 in Fig. 9B) increases the particle near-wall residence time and induce particle deposition. Particle deposition shape is a result of the balance between the hydrodynamic force generated by the angular velocity of the recirculation region and the magnetic field intensity generated by the used permanent magnet (Fig. 9B and C).

The main conclusion from this analysis refers to the fact that the horizontal and vertical position of the magnet is determinant for the quality of the accumulation in the targeted region (Fig. 10).

It is evident from Fig. 10 that the carrier particles (in our case with large radius 10 μm) are captured easily in the targeted region. The conclusion that the carrier particles with larger radius used in magnetic targeting are consistent with the experimental observation made by Lübbe et al. [33].

Particle deposition shape evolution regarding deposition length and thickness during the injection time are presented in Table 5.

As it can be seen in Fig. 10, the injected FMPs are attracted to the anastomosis wall and have a very different distribution along the host artery wall. Shape characteristics like length, width, and position are directly correlated with the flow structure (stagnation point, recirculation, helical type flow motion (presented in Fig. 8), and the magnetic field intensity and field distribution.

Fig. 11 put in evidence the strong correlation of the particle deposition with the magnet position relative to the host artery wall.

As can see in Fig. 11, for the real bypass geometry (30-degree anastomosis angle), that although the particle deposition length is practically same, the shape of the deposition in the part of the host artery labeled with zone 2 changes during the injection time. It is important to point that change in the shape of the accumulation lead to different amounts of trapped particles.

Quantitative correlations between magnet distance, magnetic field induction and particle depositions, (for the same working conditions described in Fig. 11) for each investigated magnet positions are presented in Table 6.

5. Clinical perspective

In the real case of blood flow in the arteries, flowing blood components (red blood cells, leukocytes, platelets) migrate inward from the wall at a rate that increases with cell size and cell deformability [34]. Practically, it has been demonstrated that the tendency of the constituents of the blood to migrate toward the center of a perfused vessel, in decreasing order, is as follows: red cell aggregates, leukocytes, single red blood cells, and platelets (in decreasing order of the cell size) [35].

From this point of view, using a 10 μm diameter iron particles (particles with a comparable size of the red blood cells), our experiments reproduce this migration to the artery wall.

Regarding the iron particles used in our experiments:

- iron is essential for many physiological processes, but several lines of evidence suggest that iron excess may predispose to vascular disease [36].
- for example, locally enhanced vascular production of reactive oxygen species (ROS) decreases the bioavailability of nitric oxide (NO), (promoting platelet adhesion and aggregation), is a consequence of the high quantities of the body iron [37].
- On the other hand, iron oxide at different size is used as a contrast medium in MRI. Ultra-small superparamagnetic particles of iron oxide (USPIO) due to of their small size (≈30 nm) is used successfully in medical practices because they extravasate freely through

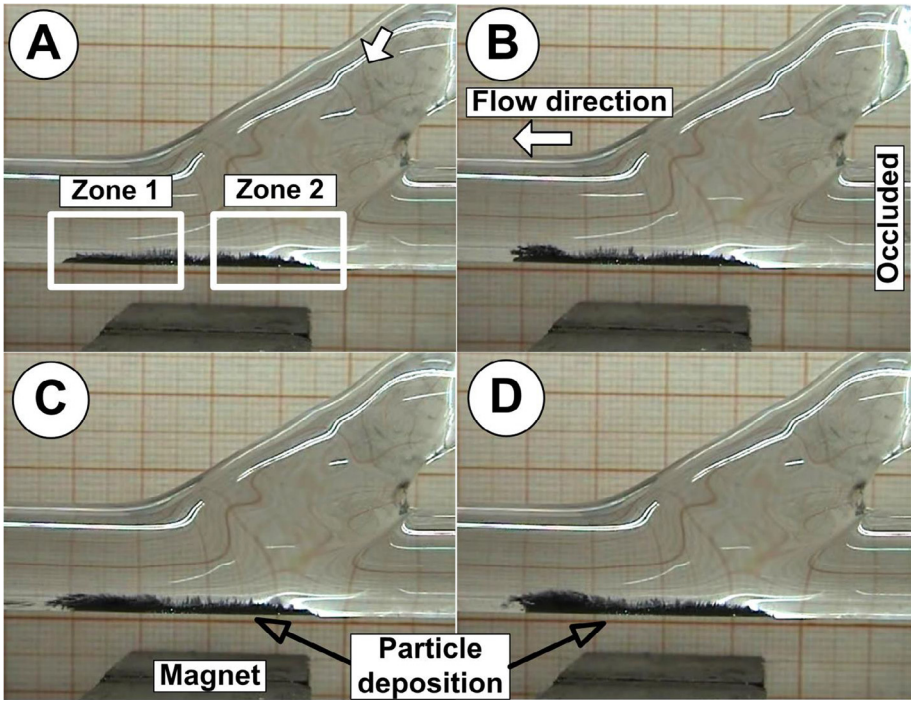

Fig. 10. Particle retention in the bypass anastomosis region during the injection time of the 30 s. The distance between the permanent magnet and bypass wall are 5 mm. The average intensity of the magnetic field along the bypass bottom wall was B = 0.11 T according to Fig. 6. Particle deposition at the different time steps: A) T = 10 s, B) T = 20 s, C) T = 25 s, D) T = 30 s (end injection).

Table 5
Characteristics of the particle accumulation shape during the injection time.

Time step [s]	Accumulation length [mm]	Average thickness corresponding to the Zone 1 [mm]	Average thickness corresponding to the Zone 2 [mm]	Magnetic field magnitude [T]
T_1 = 10	36	1	1	0.11
T_2 = 20	36	1.2	1	0.11
T_3 = 25	37	1.5	1	0.11
T_4 = 30	36	2	1	0.11

*Effective quantitative measurements of the particle accumulation it is not performed for each time steps.

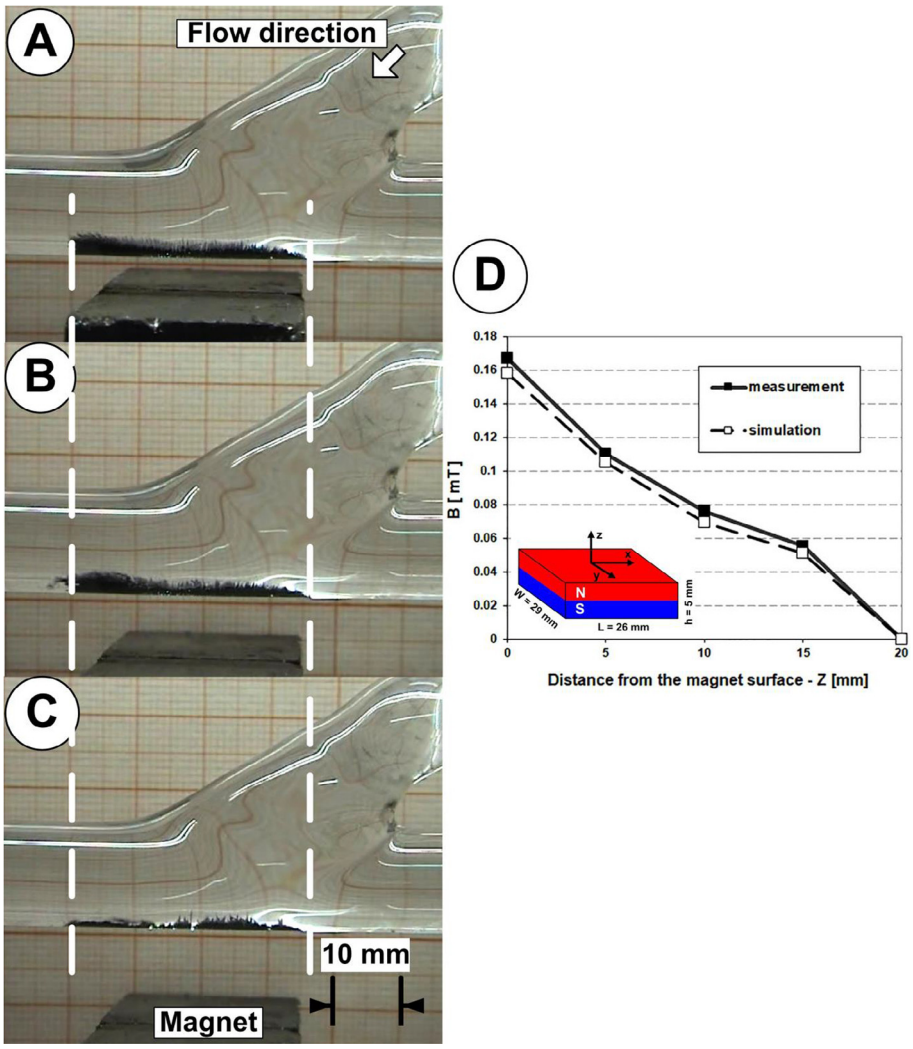

Fig. 11. Particle accumulations in the anastomosis region for different magnet position. A) Magnet distance of 2 mm, B) Magnet distance of 5 mm, C) Magnet distance of 10 mm. D) Magnetic field induction the distance to the magnet surface along to axis Z. The same working condition was applied for all magnet positions: 30-degrees anastomosis angle, inlet velocity of 0.2 m/s, and injection time of the 30 s.

Table 6
Characteristics of the particle accumulation for different magnet distance.

Magnet distance [mm]	Magnetic field magnitude [T]	Accumulation length [mm]	Particle quantity [g]
2	0.14	36	0.0321
5	0.11	36	0.0267
10	0.07	36	0.0153

capillaries and can accumulate in the cells of the spleen, liver, lymph nodes and bone marrow [38].

Taking to account all this aspect regarding to iron particles we keep in mind that in present investigations, the 10 μm diameter iron particle was used only to model the magnetic carrier in experimental investigation (not intended for clinical use), to demonstrate the feasibility of the magnetic drug targeting as a potential alternative method for effective treatment of the bypass graft intimal hyperplasia.

As it was described in Section 2.1, the anastomotic section is manufactured from glass tubing. The glass tube wall was impermeable. In reality, the human blood vessels are tortuous and arterial walls are not smooth. In this condition, driving magnetic particles in the targeted region would be hindered by particles sticking to arterial walls in the same way they stick to the current experimental setup. When planning a magnetic drug targeting treatment is essential to consider this effect, and take to account this effect for errors estimation, regarding to the

accumulated particles quantities.

In the next step, we will use particles with a good biocompatibility profile and most appropriate dimension to clinical practices, for example: coated nanoparticle (polyethylene glycol - PEG coated magnetic nanoparticle). Also, we intend to investigate a more realistic bypass model using an elastic permeable wall.

6. Conclusions

Based on experimental results, the following general features of the flow field can be identified:

- from the graft tube, a core fluid enters in the anastomosis junction and travels towards on the bed of the host tube;
- presence of the stagnation point, split flow structure into forwarding and retrograde components. Both structures induce a large near-wall velocity fluctuation in the anastomosis region;
- strong recirculation region is developed between main flow jet and occluded part of the proximal host artery;
- this vortex rotated anti-clockwise and induce a more significant exchange of fluid between the occluded arterial section and the graft; also, the recirculation region structure increases due to the contact between the main flow and the graft surface.

The character of the compound vortex structures created in the anastomosis region influence the particles deposition in the targeted region. The unstable character of the primary vortex dictates the shape of the particles accumulation in the proximal part of the anastomosis region. The different distribution along the host artery wall of the accumulated particles is due to the magnetic field distribution in the targeted region, practically depend on the horizontal and vertical positions of the magnet. The presence of the complex flow structure induces the washing effect for part of the injected particles.

Using the 10 μm diameter iron particle, we put in evidence the blood constituents migration to the artery wall for the specific flow pattern in the bypass graft anastomosis and highlight some accumulation characteristics like deposition length and accumulation position (a function of the magnetic field position and magnitude).

Acknowledgments

For S.I. Bernad this work was partially supported by the CFATR/LHC 2016–2020 research programme, and partially by a mobility grant of the Romanian Ministry of Research and Innovation, CNCS-UEDISCDI, project number PN-III-P1-1.1-MC-2018-0234. For E.S. Bernad and L. Vekas this work was supported by the grant of the Romanian National Authority for Scientific Research and Innovation, CNCS/CCCDI – UEFISCDI, project number PN-III-P2-2.1-PED-2016-0293.

Appendix A. Supplementary data

Supplementary data to this article can be found online at https://doi.org/10.1016/j.jmmm.2018.11.108.

References

[1] T.M. Kieser, G.M. FitzGibbon, W.J. Keon, Sequential coronary bypass grafts: long-term follow-up, J. Thorac. Cardiovasc. Surg. 91 (1986) 767–772.
[2] N.H. Staalsen, The anastomosis angle does change the flow fields at vascular end-to-side anastomoses in vivo, J. Vasc. Surg. 21 (1995) 460–471.
[3] V.S. Sottiurai, S.L. Sue, Ii E.L. Feinberg, W.L. Bringaze, A.T. Tran, R.C. Batson, Distal anastomotic intimal hyperplasia: biogenesis and etiology, Eur. J. Vasc .Surg. 2 (1988) 245–256.
[4] V.S. Sottiurai, Distal anastomotic intimal hyperplasia: histo-cytomorphology, pathophysiology, etiology, and prevention, Int. J. Angiol. 8 (1999) 1–10.
[5] PREVENT IV Investigators, Efficacy and safety of edifoligide, an E2F transcription factor decoy, for prevention of vein graft failure following coronary artery bypass graft surgery: PREVENT IV: a randomized controlled trial, JAMA 294 (2005) 2446–2454.
[6] S.C. Owen, H. Li, W.G. Sanders, A.K. Cheung, C.M. Terry, Correlation of tissue drug concentrations with in vivo magnetic resonance images of polymer-drug depot around the arteriovenous graft, J. Control. Release 146 (2010) 23–30.
[7] T. Rajathurai, S.I. Rizvi, H. Lin, G.D. Angelini, A.C. Newby, G.J. Murphy, Periadventitial rapamycin-eluting microbeads promote vein graft disease in long-term pig vein into-artery interposition grafts circulation, Cardiovasc. Interv. 3 (2010) 157–165.
[8] M.C. Serrano, A.K. Vavra, M. Jen, M.E. Hogg, J. Murar, J. Martinez, L.K. Keefer, G.A. Ameer, M.R. Kibbe, Poly(diol-co-citrate)s as novel elastomeric perivascular wraps for the reduction of neointimal hyperplasia, Macromol. Biosci. 11 (2011) 700–709.
[9] S.I. Bernad, A.F. Totorean, L. Vekas, Particles deposition induced by the magnetic field in the coronary bypass graft model, J. Magn. Magn. Mater. 401 (2016) 269–286.
[10] S.I. Bernad, A. Bosioc, E.S. Bernad, M.L. Craina, Comparison between experimentally measured flow patterns for straight and helical graft, Bio-Med. Mater. Eng. 24 (2014) 853–860.
[11] A.F. Totorean, A.I. Bosioc, S.I. Bernad, R. Susan-Resiga, Critical flow region in the coronary bypass graft anastomosis, Proc. Romanian Acad. Series A 16 (2) (2015) 201–208.
[12] A. Latib, L. Ferri, A. Ielasi, J. Cosgrave, C. Godino, E. Bonizzoni, E. Romagnoli, A. Chieffo, M. Valgimigli, C. Penzo, M. Carlino, I. Michev, G.M. Sangiorgi, M. Montorfano, F. Airoldi, A. Colombo, Comparison of the long-term safety and efficacy of drug-eluting and bare-metal stent implantation in saphenous vein grafts, Circ. Cardiovasc. Interv. 3 (2010) 249–256.
[13] P. Meier, E.S. Brilakis, R. Corti, G. Knapp, M.H. Shishehbor, H.S. Gurn, Drug-eluting versus bare-metal stent for treatment of saphenous vein grafts: a meta-analysis, PLoS ONE 5 (6) (2010) e11040, https://doi.org/10.1371/journal.pone.0011040.
[14] S.V. Pislaru, A. Harbuzariu, G. Agarwal, T. Witt, R. Gulati, N.P. Sandhu, C. Mueske, M. Kalra, R.D. Simari, G.S. Sandhu, Magnetic forces enable rapid endothelialization of synthetic vascular grafts, Circulation 114 (suppl I) (2006) I-314–I-318.
[15] R. Torii, N.B. Wood, N. Hadjiloizou, A.W. Dowsey, A.R. Wright, A.D. Hughes, J. Davies, D.P. Francis, J. Mayet, G. Yang, S.A. Thom, X.Y. Xu, Stress phase angle depicts differences in coronary artery hemodynamics due to changes in flow and geometry after percutaneous coronary intervention, Am. J. Physiol. Heart Circ. Physiol. 296 (2009) H765–H776.
[16] S.I. Bernad, A.I. Bosioc, E.S. Bernad, M.L. Craina, Helical type coronary bypass graft performance: experimental investigations, Bio-Med. Mater. Eng. 26 (s1) (2015) 477–486.
[17] J.B. Segur, H.E. Oberstar, Viscosity of glycerol and its aqueous solutions, Ind. Eng. Chem. 43 (9) (1951) 2117–2120.
[18] L. Vekas, Ferrofluids and magnetorheological fluids, Adv. Sci. Technol. 54 (2008) 127–136.
[19] J. Nowak, F. Wiekhorst, L. Trahms, S. Odenbach, The influence of hydrodynamic diameter and core composition on the magnetoviscous effect of biocompatible ferrofluids, J. Phys.: Condens. Matter 26 (2014) 176004.
[20] T.G. Mezger, The Rheology Handbook, Curt R. Vincentz Verlag, Hannover, 2002.
[21] D. Susan-Resiga, D. Bica, L. Vekas, Flow behavior of extremely bidisperse magnetizable fluids, J. Magn. Magn. Mater. 322 (20) (2010) 3166–3172.
[22] Y.I. Cho, K.R. Kensey, Effects of the non-Newtonian viscosity of blood on flows in a diseased arterial vessel. Part 1: Steady flows, Biorheology 28 (3–4) (1991) 241–262.
[23] H. Samady, P. Eshtehardi, M.C. McDaniel, J. Suo, S.S. Dhawan, C. Maynard, L.H. Timmins, A.A. Quyyumi, D.P. Giddens, Coronary artery Wall Shear Stress is associated with progression and transformation of atherosclerotic plaque and arterial remodeling in patients with coronary artery disease, Circulation 124 (2011) 779–788.
[24] R.K. Banerjee, K.D. Ashtekar, T.A. Helmy, M.A. Effat, L.H. Back, S.F. Khoury, Hemodynamic diagnostics of epicardial coronary stenoses: in-vitro experimental and computational study, BioMed. Eng. OnLine 7 (24) (2008), https://doi.org/10.1186/1475-925X-7-24.
[25] S. Laurent, A.A. Saei, S. Behzadi, A. Panahifar, M. Mahmoudi, Superparamagnetic iron oxide nanoparticles for delivery of therapeutic agents: opportunities and challenges Expert Opinion, Drug Delivery 11 (9) (2014) 1–22.
[26] L.H. Reddy, J.L. Arias, J. Nicolas, P. Couvreur, Magnetic nanoparticles: design and characterization, toxicity and biocompatibility, pharmaceutical and biomedical applications, Chem. Rev. 112 (2012) 5818–5878.
[27] M. Diez-Silva, M. Dao, J. Han, C.T. Lim, S. Suresh, Shape and biomechanical characteristics of human red blood cells in health and disease, MRS Bull. 35 (5) (2010) 382–388.
[28] R. Jurgons, C. Seliger, A. Hilpert, L. Trahms, S. Odenbach, C. Alexiou, Drug loaded magnetic nanoparticles for cancer therapy, J. Phys.-Condens. Matter 18 (2006) S2893–S2902.
[29] A.S. Lübbe, C. Bergemann, W. Hunt, T. Fricke, H. Riess, J.W. Brock, D. Huhn, Preclinical experiences with magnetic drug targeting: tolerance and efficacy, Cancer Res. 56 (1996) 4694–4701.
[30] K. Schulze, A. Koch, B. Schopf, A. Petri, B. Steitz, M. Chastellain, M. Hofmann, H. Hofmann, B. von Rechenberg, Intraarticular application of superparamagnetic nanoparticles and their uptake by synovial membrane—an experimental study in sheep, J. Magn. Magn. Mater. 293 (2005) 419–432.
[31] M.O. Aviles, A.D. Ebner, J.A. Ritter, Implant assisted-magnetic drug targeting: comparison of in vitro experiments with theory, J. Magn. Magn. Mater. 320 (2008) 2704–2713.
[32] E. Allan, D.J. Adam, C.B. Chertok, Y.S. Park, V.C. Yang, A combined theoretical and in vitro modeling approach for predicting the magnetic capture and retention of magnetic nanoparticles in vivo, J. Control. Release 152 (2011) 67–75.

[33] A.S. Lübbe, C. Bergeman, H. Riess, F. Schriever, P. Reichardt, K. Possinger, M. Matthias, B. Dörken, R. Gürtler, P. Hohenberger, N. Haas, R. Sohr, B. Sander, A. Lemke, D. Ohlendorf, W. Huhnt, D. Huhn, Clinical experiences with magnetic drug targeting: a phase I study with 4′-epidoxorubicin in 14 patients with advanced solid tumors, Cancer Res. 56 (1996) 4686–4693.
[34] T. Watts, M. Barigou, G.B. Nash, Comparative rheology of the adhesion of platelets and leukocytes from flowing blood: why are platelets so small? Am. J. Physiol. Heart Circ. Physiol. 304 (2013) H1483–H1494.
[35] A.A. Palmer, Platelet and leucocyte skimming, Bibliotheca Anat. 9 (1967) 300–303.
[36] M.S. Day, D. Duquaine, L.V. Mundada, R.G. Menon, B.V. Khan, S. Rajagopalan, W.P. Fay, Chronic iron administration increases vascular oxidative stress and accelerates arterial thrombosis, Circulation 107 (2003) 26012606.
[37] G. Russo, J.A. Leopold, J. Loscalzo, Vasoactive substances: nitric oxide and endothelial dysfunction in atherosclerosis, Vasc. Pharmacol. 38 (2002) 259–269.
[38] R.S. Alam, A.S.V. Shah, J. Richards, N.N. Lang, G. Barnes, N. Joshi, T. MacGillivray, G. McKillop, S. Mirsadraee, J. Payne, K.A.A. Fox, P. Henriksen, D.E. Newby, S.I.K. Semple, Ultrasmall superparamagnetic particles of iron oxide in patients with acute myocardial infarction early clinical experience, Circ. Cardiovasc. Imag. 5 (2012) 559–565.